Enhancing SWAT with remotely sensed LAI for improved modelling of ecohydrological process in subtropics

Tianxiao Ma[a,b], Zheng Duan[c], Runkui Li[a,d,] Xianfeng Song[a,b,d]*

[a] *College of Resources and Environment, University of Chinese Academy of Sciences, Beijing 100049, China*

[b] *Sino-Danish College, University of Chinese Academy of Sciences, Beijing 100049, China*

[c] *Chair of Hydrology and River Basin Management, Technical University of Munich, Arcisstrasse 21, 80333 Munich, Germany*

[d] *State Key Laboratory of Resources and Environmental Information System, Institute of Geographic Sciences and Natural Resources Research, Chinese Academy of Sciences, Beijing, 100101, China*

* Corresponding author:

Xianfeng Song, Professor

College of Resources and Environment, University of Chinese Academy of Sciences, Beijing 100049, China

Tel.: +86 10 69672967

E-mail: xfsong@ucas.ac.cn

Enhancing SWAT with remotely sensed LAI for improved modelling of ecohydrological process in subtropics

Abstract:

Vegetation growth in Soil and Water Assessment Tool (SWAT) is a crucial process for quantifying ecohydrological modelling, as it influences evapotranspiration, interception, soil erosion and biomass production. The simplified version of Environmental Policy Integrated Climate (EPIC) in SWAT was originally designed for temperate regions and naturally based on temperature to simulate growth cycles of vegetation. However, tropical or subtropical vegetation growth is mainly controlled by rainfall. Due to this limitation, current SWAT simulations in tropics and subtropics have been facing a series of problems on vegetation dormancy, water balance and sediment yield. Therefore, we proposed an approach to enhance the modelling of SWAT vegetation dynamics with remotely sensed leaf area index (LAI), to finally increase the applicability of SWAT in tropical or subtropical areas. Spatially and temporally continuous LAI products (1day, 500m) from Moderate Resolution Imaging Spectroradiometer (MODIS) observations were integrated into SWAT to replace the LAI simulated by built-in EPIC module. Two advanced filter algorithms were employed to derive a downscaled LAI (30m) to keep a consistent spatial scale with the size of Hydrological Response Units (HRU) and open data (i.e. SRTM, 30m), and the source code of the plant growth module were correspondingly modified to incorporate the downscaled LAI into SWAT. To examine the performance of our proposed approach, a case study was conducted in a representative middle-scale (6384km^2) subtropical watershed of Meichuan basin, China, and detailed analysis was performed to investigate its ecohydrological effects, such as streamflow, sediment yield and LAI dynamics from 2001 to 2014. Model performances were compared among three scenarios: (1) original SWAT, (2) SWAT with a corrected plant dormancy function, and (3) modified SWAT after integration of MODIS LAI (our proposed method). Results showed that the modified SWAT took advantage of downscaled MODIS LAI and produced more reasonable seasonal curves of vegetation cover factor (C) of plants than the original model. Correspondingly, the modified SWAT substantially improved streamflow and sediment simulations. The findings demonstrated that SWAT model can be a useful tool for simulating ecohydrological process for subtropical ecosystems when integrated with our proposed method.

Keywords: Vegetation growth, Subtropics, LAI, MODIS, Integration, Modified SWAT

1 Introduction

Vegetation growth inevitably coincides with an important ecohydrological process influenced by water availability and feeds back to affect regional water balance (Yang et al., 2009; Berghuijs et al., 2015). For rainfall, canopy often intercepts precipitation as a water storage and hinders water drops to reduce splash erosion by the loss of speed (Hilker et al., 2014). Vegetation may also reduce overland flow speed, increasing infiltration time and resulting in soil deposit on ground surface. (Liu et al., 2018). For evaporation, vegetation functions like a bump that transports soil water even shallow aquifer into atmosphere. (Stephenson, 1998). These alterations often play a vital role on the spatial and temporal dynamics of streamflow and sediment production and transportation (Guzha et al., 2018). Thus, detailed simulation of vegetation growth is critical for water balance and will be useful for the explanation of many interactions in hydrological processes such as streamflow and sediment (Li et al., 2013; Mwangi et al., 2016).

The Soil and Water Assessment Tool (SWAT; Arnold et al., 1998) is a process-oriented, semi-distributed and time-continuous river basin model that combines a plant growth module to simulate streamflow and sediment under a range of climate and management conditions (Arnold et al., 2012; Bressiani et al., 2015). SWAT has been widely used in modeling hydrological processes (e.g. streamflow, surface runoff, evapotranspiration and sediment) and vegetation dynamics such as leaf area index, crop yield and biomass (Kauffman et al., 2014; Glavan et al., 2015; Mekonnen et al., 2017). However, only a few studies have considered the limitations of simulating vegetation dynamics and evaluated the performance of plant growth module (Wagner et al., 2011; Francesconi et al., 2016).

In SWAT, the plant growth module is a simplified version of Environmental Policy Integrated Climate (EPIC) crop growth model, which was originally developed to assess the effect of erosion on soil productivity (Williams et al., 1989; Neitsch et al., 2011). It uses EPIC concepts to model plant growth which based on heat units to simulate leaf area development, light interception, and conversion of the intercepted light into biomass (Lychuk et al., 2015). Therefore, the Leaf Area Index (LAI), which is defined as the area of green leaves per area of land, plays a key role in SWAT for further estimating other processes, such as evapotranspiration and biomass accumulation (Ren et al., 2010; Almeida et al., 2011). Due to the shortcomings of EPIC model in subtropical regions, there are two potential problems that generate uncertain estimates of the LAI values, as already noted in previous studies (Anderson et al., 2002; Strauch and Volk, 2013).

First, plant growth dynamics are originally controlled only by the temperature in SWAT model, which is inapplicable to subtropical regions where precipitation is a primary controlling factor for both leafing and senescence (Jolly and Running 2004; Pfeifer et al., 2014). Several studies also pointed out that there was a significant mismatch between SWAT simulated LAI and remote-sensing based estimates in subtropical watersheds, and they suggested that plant growth module was needed to be critically examined for appropriate use (Plesca et al., 2012). To solve these problems resulting from unrealistic presentation of LAI, previous studies mostly considered soil moisture as an indicator to initiate subtropical plant growth in SWAT (Strauch and Volk, 2013; Alemayehu et al., 2017). Although an improved simulation of the seasonal dynamics of the LAI was obtained, the simulated LAI by SWAT still was found to be considerably inconsistent with the Moderate Resolution Imaging Spectroradiometer (MODIS) 8-day LAI (Alemayehu et al., 2017). As input to a hydrological model like SWAT, remotely sensed LAI has a great potential for enhanced presentation of land surface parameters in a broad area and make vegetation dynamics more realistic (Zhang & Wegehenkel, 2006; Sun et al., 2018). Compared to field measured LAI and soil moisture-based LAI, remotely sensed LAI product has its advantages for providing spatially and temporally continuous information for improving predictive accuracy of SWAT models.

Second, daylength driven dormancy was applied in SWAT plant growth module to repeat the annual growth cycle for trees and perennials (Wagner et al., 2011). Dormancy assumes that plants do not grow as daylength nears the shortest daylength for the year (Arnold et al., 1998; Trybula et al., 2015). However, plants do not have a dormant period in the subtropics and tropics. The SWAT plant growth dynamics could not reflect the physical reality in tropical area by assuming LAI sharply drops to a very low level at the end of year. A general approach to addressing this issue is shifting the dormancy period by editing crop database or LAI curve controlling parameters (Wagner et al., 2011; Strauch and Volk, 2013). This method might avoid dormancy to some degree in subtropical areas, but the default dormancy could not be authentically removed without modifying the SWAT source code.

In this study, we take advantages of MODIS LAI which has been proven capable of monitoring vegetation timely and accurately at a large scale and easy to obtain (Yuan et al, 2011). MODIS LAI values were firstly improved by using time series filter and downscaling. Afterwards, MODIS LAI were incorporated into SWAT through hydrological response units (HRUs) to replace the originally simulated LAI, and other parameters such as biomass and C factor (cover and management factor used in modelling sediment) were consequently updated based on the observed LAI. Meanwhile, the drawbacks of dormancy that affecting representation of vegetation change were completely overcome by modifying the dormancy function of daylength and latitude in SWAT source code. Performance of SWAT with revised plant growth module was evaluated for simulating streamflow and sediment yield in a typical subtropical watershed.

The specific objectives of this study are to: (1) obtain high spatial resolution and temporally continuous satellite-based LAI that can reasonably represent vegetation dynamics in HRU level; (2) improve the predictive capability of SWAT by modifying plant growth module to integrate remotely sensed LAI into SWAT; and (3) explore the variations of vegetation-related parameters and their rationalities in the changed plant growth module.

2 Theoretical Background

The plant growth module of SWAT is a simplification of EPIC model, which simulates the vegetation growth based on daily cumulative heat units (Williams et al., 1989; Neitsch et al., 2011). It assumes that plant growth only occurs on the days when daily mean temperature exceeds the base temperature for growth (Kiniry and MacDonald, 2008). This means that temperature is the main governing factor of plant growth in SWAT.

Derived from temperature requirements (i.e. minimum, maximum and optimum for growth), heat units (HU) is an index that is applied to measure the heat acquirements of a plant and calculated as follows (Arnold et al, 1998):

$$HU = \bar{T}_{av} - T_{base} \quad when \;\; \bar{T}_{av} > T_{base} \tag{1}$$

where HU, $\bar{T}_{av}$ (℃) and T_{base} (℃) are the values of heat units accumulated on a given day, mean daily temperature and base temperature, respectively. Consequently, the required HU for plant maturity can be computed as the following equation:

$$PHU = \sum_{d=1}^{m} HU \tag{2}$$

where PHU (Potential Heat Units) refers to the total heat units required for plant maturity; d is the number of day ($d = 1$ is the day of starting planting); m is the number of days required for a plant to reach maturity. It is worthwhile noting that PHU is known before model running and is given in model database. Thus, a fundamental variable for computing LAI could be produced by:

$$fr_{PHU} = \frac{\sum_{i=1}^{d} HU_i}{PHU} \tag{3}$$

where fr_{PHU} is the fraction of potential heat units for a certain period during the growing season. When plants reach maturity, fr_{PHU} will be 1.

Corresponding to a given fraction of the potential heat units, the function of optimal leaf area development is listed as:

$$fr_{LAImx} = \frac{fr_{PHU}}{fr_{PHU} + \exp(l_1 - l_2 \cdot fr_{PHU})} \tag{4}$$

where fr_{LAImx} is the fraction of the plant's maximum leaf area index for the plant; l_1 and l_2 are shape coefficients. For plants, the increase of LAI on a day i is calculated as:

$$\Delta LAI_i = (fr_{LAImx,i} - fr_{LAImx,i-1}) \cdot LAI_{mx} \cdot (1 - \exp(5 \cdot (LAI_{i-1} - LAI_{mx}))) \tag{5}$$

which is used to derive the LAI for the day:

$$LAI_i = LAI_{i-1} + \Delta LAI_i \tag{6}$$

where ΔLAI_i is the change of LAI on day i; $fr_{LAImx,i}$ and $fr_{LAImx,i-1}$ are the fraction of the plant's maximum leaf area index for the day i and $i-1$, respectively; Similarly, LAI_i and LAI_{i-1} are the leaf area index for the the day i and $i-1$; LAI_{mx} is the maximum leaf area index for the plant.

Depending on the LAI, a series of critical parameters related to streamflow and sediment are determined. For instance, C factor (cover and management factor) is one of the important factors of the Modified Universal Soil Loss Equation (MUSLE) in SWAT to model sediment yield (Wischmeier and Smith, 1978). C factor used in SWAT is a function of the amount of residue on the soil surface, which is also obtained from LAI (Song et al., 2011). In addition, parameters such as biomass and the amount of baseflow and surface runoff would be changed when LAI values are adjusted (Qiao et al., 2015).

3 Materials and Methods

3.1 Study area

The Meichuan Basin, a representative basin of Poyang Lake, is located between 26° 00′-27°09′N and 116°36′-116°39′E in Jiangxi Province, southeastern China (Fig.1). It has a drainage area of 6384km^2, which is an upstream tributary of Gan River contributing to Poyang Lake and the Yangtze River. The elevation ranges from 137 to 1425m, with a mean of 358m. This watershed has a subtropical wet climate characterized by an annual mean temperature of 17℃ and annual mean precipitation of 1628 mm during study period from 2001 to 2014. The land use of Meichuan Basin is diversified with a dominant forest (40.63%) and secondary cropland (27.19%). The cropping system is two seasonal crops per year and the cultivation consists largely of rice. The main soil types are red soil and paddy soil, covering 64.3% and 28.2% of total area, respectively.

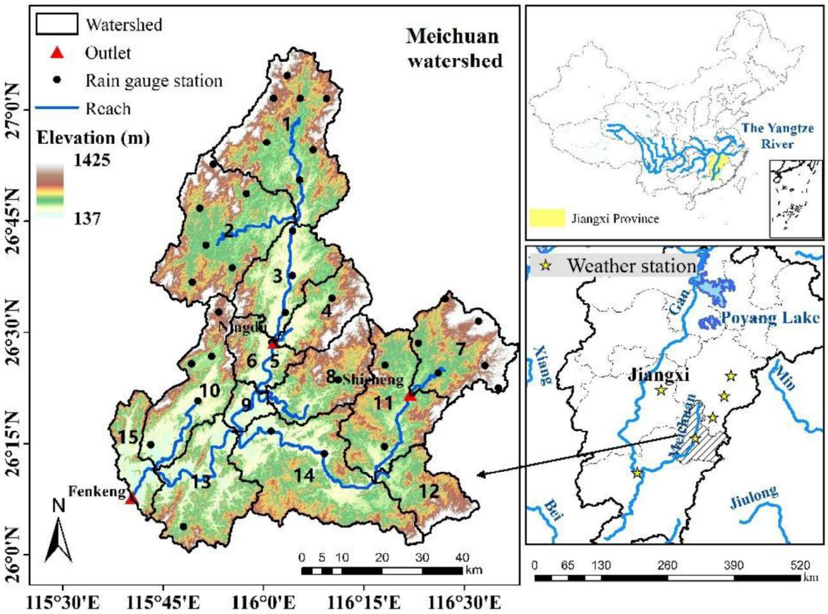

Fig.1. Locations of climate stations, rain gauge stations and subbasins in Meichuan Basin

3.2 Datasets and SWAT settings

The data sources used in this research are as listed in Table 1. By combining the knowledge of soil–landscape relationships with geographic information systems under fuzzy logic, the detailed soil spatial data with a spatial resolution of 30 m were generated from the original 1: 500 000 soil maps using the Soil Land Inference Model (Zhu et al., 2001). Observed daily streamflow and sediment for the watershed outlet (gauge Fenkeng) and daily rainfall of the study area was obtained from the Chinese Hydrological Data Yearbook from 2001 to 2014. Data of six climate station were obtained from CMDC (Chinese Meteorological Data Service Center), including daily temperature, solar radiation, humidity and wind speed.

Table 1 The SWAT model datasets for Meichuan Basin

Data Type	Spatial/Temporal Resolution	Source
Digital Elevation Model (DEM)	30 m	ASTER GDEM
Land use	30 m	FROM-GLC (Finer Resolution Observation and Monitoring of Global Land Cover, Gong et al., 2013, http://data.ess.tsinghua.edu.cn/fromglc2015_v1.html)
Soil	30 m	Generated from 1:500000 soil vector maps (downloaded from Resources and Environment Data Cloud Platform, http://www.resdc.cn/Default.aspx)
Rainfall	Daily (2001-2014)	Chinese Hydrological Data Yearbook
Climate	Daily (2001-2014)	CMDC (Chinese China Meteorological Data Service Center)
Streamflow	Daily (2001-2014)	Chinese Hydrological Data Yearbook
Sediment	Daily (2001-2014)	Chinese Hydrological Data Yearbook
LAI	8 days/500m	MCD15A2H
Landsat	16 days/30m	Landsat 5,7,8

The MODIS Collection 5 LAI (MCD15A2H) global products were downloaded from https://e4ftl01.cr.usgs.gov/MOLT/MCD15A2H.006/ and used in this study for fourteen years' vegetation growth simulation during 2001-2014 period. The product is composited every 8 days at 500m resolution and its retrieval algorithm is based on a three-dimensional radiation transfer model (Knyazikhin et al., 1998) using different sets of canopy realization and view geometry as inputs. Available Landsat-5 TM, Lantsat-7 ETM+ and Landsat-8 scenes (30m) acquired in different years were also downloaded from Geospatial Data Cloud (http://www.gscloud.cn/), amounting to a total of 181 scenes for establishing the relationship in downscaling method. To investigate the effect of different vegetation types with modified SWAT model on hydrological processes, the LAI was separated into six land use categories: cropland, grassland, shrubland, evergreen forest, deciduous forest and mixed forest. Management practices of cropland (Supplementary Material Table S1) used as input in the model were derived from information provided by Li et al. (2013). Management practices of other plants were scheduled as default in management database of SWAT.

SWAT2012 (revision 664) was set up for Meichuan Basin to model streamflow and sediment. Based on DEM, the Meichuan Basin was delineated into 15 sub-basins and 419 HRUs (Fig.1). The first 2 years were used as warm-up period to mitigate the initial conditions and were excluded from the analysis (2001-2002). The SWAT model was calibrated at monthly time step from 2003 to 2010 and validated from 2011 to 2014 based on streamflow observations. In this basin, three hydrological gauges (Shicheng, Ningdu and Fenkeng) provide measured streamflow data for the investigated period, but only one hydrological gauge (Fenkeng, outlet of this basin) has continuous measured sediment data. Therefore, there will be a different number of calibration and validation between streamflow and sediment to understand the physical behaviors in upstream and downstream flow.

3.3 Integration of remotely sensed LAI into SWAT

Several studies demonstrated that methods applied in SWAT plant growth module are not suitable for subtropical areas because of controlling factor and dormancy (Wagner et al., 2011; Strauch and Volk, 2013; Alemayehu et al., 2017). Thus, we proposed to integrate remotely sensed LAI time series into SWAT plant growth module to replace the LAI simulated by SWAT. With this, actual vegetation dynamics can be reflected and the occurrence of dormancy during plant growth is also avoided. Consequently, a specific approach to MODIS LAI process and SWAT revision was developed in this study, details are described in the following subsections.

3.3.1 Filtering MODIS LAI time series products

MODIS LAI products have been widely used for its long-term record and character of high temporal resolution (Fang et al., 2008). However, there are significant discontinuity and noise in MODIS LAI products due to cloud and snow cover, as well as instrument failure (Weiss et al., 2007; Li et al., 2009). To obtain the continuous and smooth dynamic that was required by SWAT modelling, time series filter processing thus becomes an important ingredient of a biophysical algorithm. Among several time-series filter approaches, modified Temporal Spatial Filter (mTSF) was selected in our study due to its specific adaption for estimating vegetation indices such as LAI (Yuan et al., 2011).

The mTSF was performed pixel by pixel for all the fourteen years data. The procedures can be divided into three main steps: (1) Calculating the background value.

For each pixel of MODIS LAI product, there is quality control (QC) information restored as 8-bit data to reflect the corresponding algorithm and state of cloud. If the QC information indicate a good quality, e.g. a value is retrieved by main algorithm without clouds, the value will be chosen to calculate multi-year mean value which was later assigned as the background value of this pixel. (2) Filling the gaps between the observation values. If the QC information indicate that value is not retrieved by main algorithm or cloud presents, the value will be filled with the background value calculated in the first step. Missing data in time series were filled by linear interpolation independently. (3) Obtaining a final target value by applying filter. Using the results from above steps, the target value was obtained by applying Adaptive Savitzky–Golay filter (Chen et al., 2004). All processing steps have been streamlined for automatic execution based on Python and 644 MODIS images were processed.

3.3.2 Downscaling MODIS LAI products

SWAT predominantly relies upon discretizing landscapes based on common soil, land use and slope characteristics, known as hydrologic response units (HRUs; Arnold et al; 1998). To a large degree, the spatial resolution of HRUs is dependent upon the spatial resolution of input data sets, herein including the 30m grid data of DEM, landuse and soil map (Zhou et al, 2015). The 500m MODIS LAI is not appropriate to monitor detailed variations of vegetation types across space because of its inadequate spatial resolution (Giambelluca et al., 2009). It is too coarse to match the above HRU scale and raise an issue of mixing several types of distinct vegetation, that is, a MODIS LAI grid (500m) may span one more HRUs (Starks & Moriasi, 2009).

To overcome the aforementioned limitation, MODIS LAI products need to be downscaled from the medium resolution to the high-resolution scale (30m) by relying on high spatial resolution satellite imagery data such as Landsat. Spatial and Temporal Adaptive Fusion Model (STARFM) is a downscaling method that is designed to utilize the relationship between the surface reflectances of MODIS and Landsat and preserve the high spatial resolution of Landsat and the high frequency of MODIS (Emelyanova et al., 2013; Jarihani et al., 2014; Houborg et al., 2016). In this study, we proposed to implement a revised version of STARFM (Gao et al., 2006) to achieve this goal.

The processing steps of revised STARFM include: (1) Unsupervised classification for different land cover. Using Landsat image as input, the land cover classification is conducted automatically based on the unsupervised ISODATA technique. (2) Resampling. MODIS reflectance (MOD02) and LAI (MCD15) product (500m) are resampled to the fine resolution of Landsat (30m). (3) Establishment of MODIS-Landsat relationship. For each 8-day MODIS composite, MODIS-Landsat linear relationships between MODIS and Landsat surface reflectance for different land covers are established at the 30m scale. Only MODIS pixels with best quality information (QC information indicate that a value is retrieved by main algorithm without clouds) are used in establishing relationships. (4) Application of MODIS-Landsat relationship and STARFM algorithm for downscaling LAI. Based on spatial and spectral similarities between high and medium resolution reflectance data and a weighting function that exploits information from neighboring pixels, an initial Landsat scale LAI value can be generated from MODIS LAI product. Then, MODIS-Landsat relationships are applied to these initial values according to land cover types to obtain the final LAI values with high resolution (30m). (5) Execution of STARFM for re-constructing time continuous LAI. STARFM is implemented to blend co-registered and scale-consistent datasets of MODIS and Landsat and produce a new LAI dataset with a higher spatial resolution (30 m in this study).

3.3.3 Modifying SWAT code for loading refined LAI

In SWAT, HRU is the basic simulation unit for most of the physical processes, including water flow, nutrient and vegetation growth. To make use of high spatiotemporal resolution LAI, the source code in the growth subroutine (grow.f) related with producing LAI needs to be modified to introduce the observed LAI to the corresponding HRUs. However, the LAI derived from satellite images is pixel-based. Therefore, a geo-statistics analysis called zonal statistics is first adopted by overlaying the enhanced LAI images with HRU distribution map and the mean LAI value for each HRU is calculated every eight days. Then, a cubic spline interpolation method is applied on each HRU to interpolate daily LAI values using its 8-days interval LAI values. Finally, these interpolated daily LAI datasets are defined as the input of the modified growth subroutine.

Fig.2 shows the flowchart of source code modification in plant growth module of SWAT. As shown in Fig.2, high spatiotemporal resolution LAI was obtained from processing steps (blue dotted portion) as described in Section 2.2.1 and 2.2.2. Which was incorporated into plant growth module for each HRU to replace the LAI simulated by SWAT. According to original growth subroutine, the LAI values were estimated from several equations using radiation and the effect of stress. When remote sensing LAI were integrated, the calculation of plant growth module (grow.f; green dotted portion) would become inactive (grey portion). Finally, the plant growth module after incorporating with new LAI values provided updated biomass and parameters related to streamflow and sediment. This output would be restored in a new file for model calibration and validation, and also used for comparing with the results from the origin SWAT model.

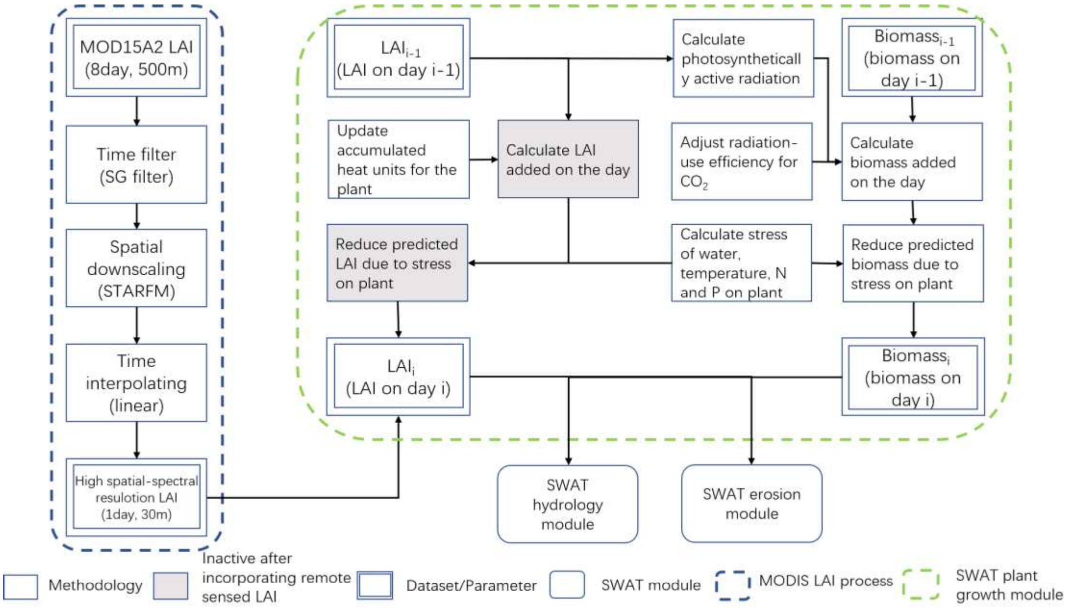

Fig.2. Flowchart of source code modification related with LAI conducted in plant growth module of SWAT

3.4 Evaluation and calibration of the modified SWAT

To evaluate the influence of SWAT modification on modeling results, three scenarios were conducted: (1) the original SWAT, (2) SWAT with a corrected dormancy function and (3) modified SWAT with refined LAI. It is worth noting that the second scenario is a modification just for dormancy issue existing in subtropical ecosystem. Unlike the original SWAT plant growth module, the second plant growth module only adopted a new dormancy function which enables to set the default time of dormancy as 0. The above three versions of SWAT were compared through their performances in simulating streamflow and sediment.

With many empirical equations for simulating physical processes within a basin, the accuracy of SWAT simulations highly depends on calibration and validation (Li et al., 2012). In this study, the parameters related to the simulation of streamflow and sediment were selected based on the one-at-a-time sensitivity analysis in SWAT-CUP (Abbaspour et al., 2015). Calibration and validation procedure were based on the SUFI-2 algorithm (Abbaspour et al., 2007) of SWAT-CUP, which is an auto-calibration and uncertainty analysis module that can deal with a number of input parameters. At first, streamflow was calibrated and validated because it is the basis of sediment simulation. In the streamflow calibration, surface runoff and baseflow were calibrated separately according to the separated components from the observed total streamflow. After streamflow calibration, sediment yield was calibrated till the evaluation metrics reached a given criteria.

Two coefficients, Nash-Sutcliffe efficiency (E_{NS}; Nash and Sutcliffe, 1970) and the coefficient of determination (R^2) were used for evaluating the fit goodness between simulated and observed estimates on both streamflow and sediment:

$$\mathrm{E}_{NS} = 1 - \frac{\sum_{i=1}^{n}(O_i - P_i)^2}{\sum_{i=1}^{n}(O_i - \bar{O})^2} \tag{7}$$

$$R^2 = \frac{\left(\sum_{i=1}^{n}(O_i - \bar{O})(P_i - \bar{P})\right)^2}{\sum_{i=1}^{n}(O_i - \bar{O})^2 \sum_{i=1}^{n}(P_i - \bar{P})^2} \tag{8}$$

where n is the number of observations; O_i and P_i are the observed and predicted value at the time i; $\bar{O}$ and $\bar{P}$ are the mean of observed and predicted values. E_{NS} represents the performance of model output in comparison with the mean of observed data. R^2 indicates the consistency of trend between the observed and simulated values.

The closer the two coefficients to 1, the better of model performance. Following existing studies (Santhi et al., 2001; Moriasi et al., 2007; Ye et al., 2018), the criteria of evaluating the model performance can be categorized into unsatisfactory performance ($\mathrm{E_{NS}} \leq 0.50 \text{ and } R^2 \leq 0.60$), satisfactory performance ($0.50 < \mathrm{E_{NS}} \leq 0.65 \text{ and } 0.60 < R^2 \leq 0.70$), good performance ($0.65 < \mathrm{E_{NS}} \leq 0.75 \text{ and } 0.70 < R^2 \leq 0.80$) and very good performance ($0.75 < \mathrm{E_{NS}} \leq 1.00 \text{ and } 0.80 < R^2 \leq 1.00$).

4 Results

4.1 High spatiotemporal resolution LAI

Fig.3 present the enhanced LAI after downscaling and shows the agreement between original MODIS (500m) and downscaled LAI (30m) at the scale of the entire basin and a typical zoom in view on August 20, 2008. As expected, much detailed spatial LAI patterns can be found in downscaled LAI but have been averaged out in original MODIS LAI. The normalized frequency distribution (Fig.3c) also indicates that an equivalent clusters exists among two downscaled and original LAIs.

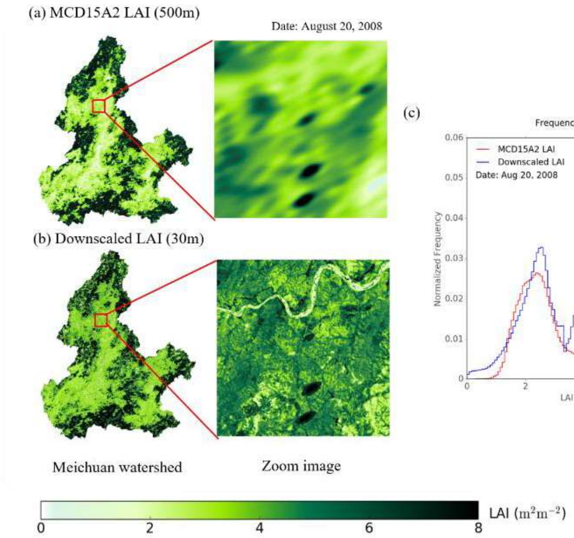

Fig.3. MCD15A2H (a) and downscaled (b) maps of LAI on August 20, 2008. The right plot (c) shows the normalized frequency distributions of these two LAI maps

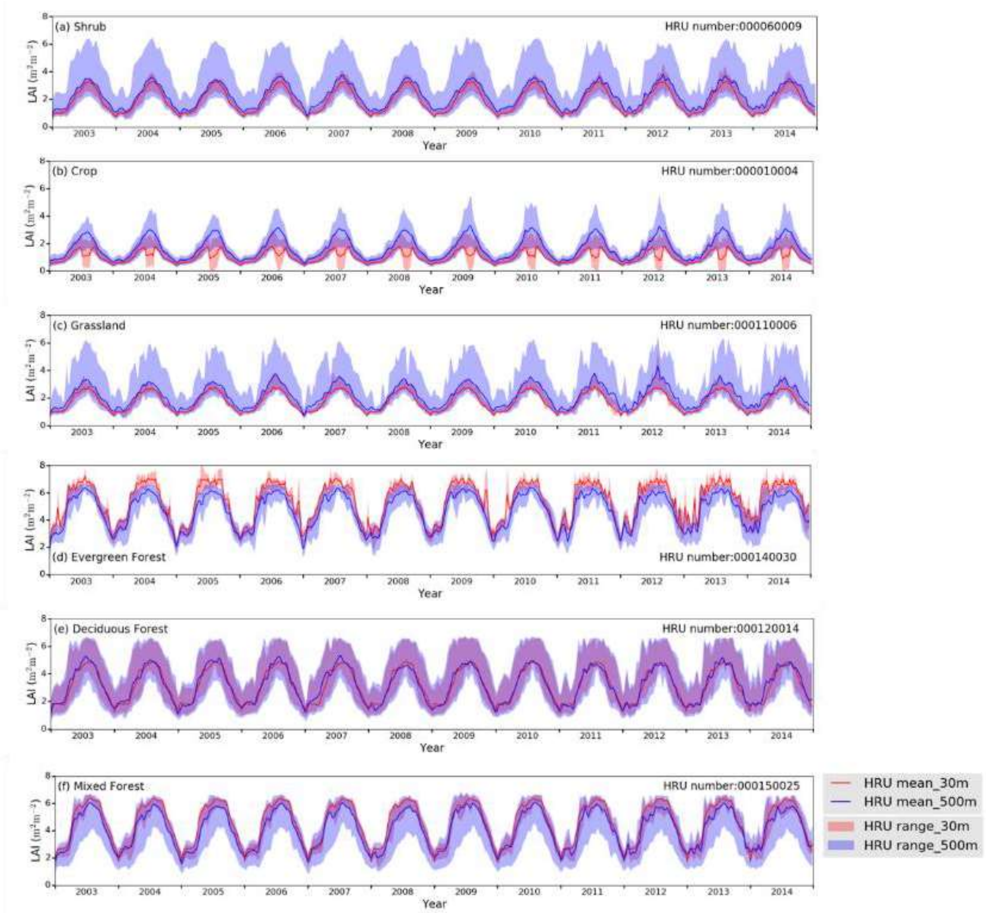

Fig.4. The daily means and ranges of original MODIS LAI (500m) and improved LAI in an HRU (30m). The shadings indicate the range of LAIs within a HRU

After reconstruction of high spatiotemporal LAI values, the dynamics of improved LAI (30m) in Meichuan Basin were generated temporally and spatially (Fig.4 and Fig.5). Fig.5 shows the improved LAI and the original MODIS LAI over several land use types at HRU level temporally. From the visual perspective, improved LAI has a more centralized range than original MODIS LAI except for deciduous forest, suggesting that improved LAI produces less abrupt fluctuations. It can be observed that the improved MODIS LAI values are much smoother than original MODIS LAI. In original products, the LAIs of evergreen, deciduous and mixed forests show unreasonable spikes and peaks in time-series. In addition, the LAIs of shrub, grass and crop with poor quality are observed mainly in growing seasons such as summer. For crop land, the improved MODIS LAI values display a slightly weak trend of double crop growth peaks after time filtering, indicating a more realistic scenario. For the grass and shrub land use types, the improved MODIS LAI values are quite similar with original ones except for the peak part during growing season. For three forest land use types, there are several negative offset effects in time series of LAI caused by the contamination of atmospheric factors.

Misrepresentative seasonal dynamics of LAI has also been corrected by downscaling to acquire a high spatial resolution. For instance, the trend of crop has been significantly changed from single-cropping to double-cropping even at a small HRU (Fig.4b). HRU means of improved LAI values of three trees were also higher than original MODIS LAI, whereas HRU means of improved LAI values were lower in other three vegetation types. This is attributed to mixed plants within a medium resolution pixel (500 m).

To display the detailed spatial characteristics of vegetation dynamics after downscaling, seasonal and spatial distribution of improved LAI (30m) at HRU level were presented in Fig.5. For seasonal changes, January and July were the months with lowest and highest LAI values, respectively. These estimates are also well reflected in the time variability of the LAI (Fig.4). From the spatial distribution shown in Fig.5, the LAI over crop regions in the middle part of the study area was persistently low throughout the year, but regions with other plant types varies largely with the change of season. The results in time and space clearly demonstrate the capability of our proposed method at providing high-accuracy LAI data for precisely describing plant growth cycle characteristics and streamflow in subtropical ecosystems.

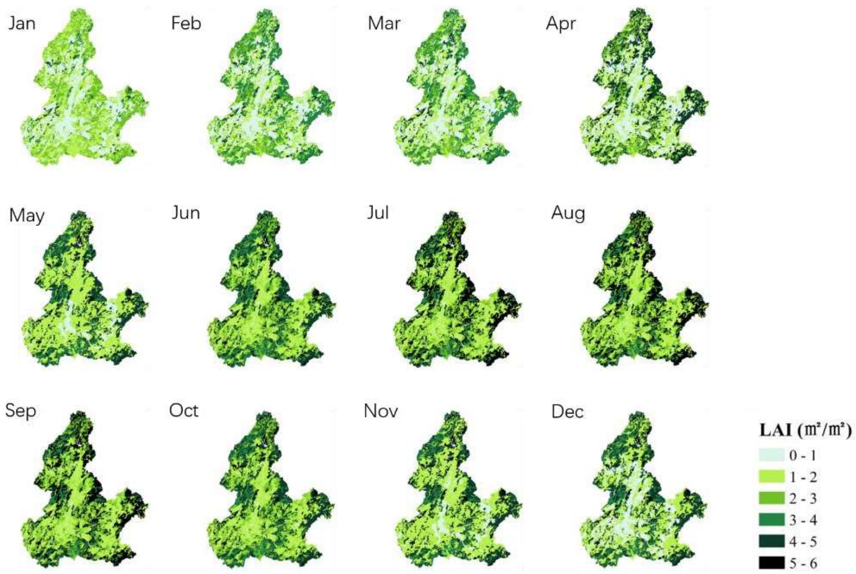

Fig.5. The spatial distribution of long-term (2001–2014) monthly averaged LAI (30m) in the Meichuan Basin at HRU level for each month.

4.2 Model performance in streamflow and sediment simulation

4.2.1 Streamflow simulation

Based on the sensitivity analysis, eight sensitive parameters were selected for streamflow calibration (Supplementary Materials Table S3). Auto-calibration was performed in three outlets for finding the optimal values of all eight parameters with different plant growth modules during 2003-2010. It is noted that ALPHA_BF (baseflow alpha factor) is a recession constant that was generated from baseflow separation program to account for sub-surface water response simulated by SWAT. The default values, calibrated values and calibrated values in combination with MODIS LAI for each parameter in the calibration process are also presented in Supplementary Materials Table S3.

For accurate analysis of water flow pathways, baseflow and surface runoff separated from the watershed were summed to predict streamflow at three outlets (Supplementary Material Fig.S2 and Table S2). The time-series plots of predicted and measured monthly streamflow at three stations during the calibration (2003-2010) and validation (2011-2014) periods are shown in Fig.6. Generally, the predicted streamflow with original and modified model during both the calibration and validation periods matched the measured streamflow. Furthermore, streamflow corresponded well to precipitation.

For designed three scenarios – the original SWAT, the dormancy corrected SWAT and the modified SWAT with MODIS LAI, all statistical evaluation criteria in Table 2 indicated three models predicted well. The dormancy occurs during late December and lasts about 7~14 days depending on vegetation types. This period belongs to dry season and has a relatively-lower precipitation. So, as shown in Table 2, the performance of Scenario-2 is a little bit better than Scenario-1 and much worse than Scenario-3. The Scenario-2 has almost same streamflow and sediment as the original model except that a slight difference might exist in December.

By observing the temporal variation of streamflow at three gauge stations, in general simulated streamflow was higher than the observed during dry season (winter and spring) except Shicheng station, which has a lowest flow among these stations. From Table 2, it can be seen that E_{NS} and R^2 ranges of baseflow for calibration were from 0.71- 0.74 and 0.73-0.8, respectively. For the validation period, the simulated and observed flows showed a very good agreement as indicated by E_{NS} (0.76-0.8) and R^2 (0.80-0.89). There seems to be smaller difference between simulated surface runoff and the observed (Supplementary Material Fig. S3 and S4). This is supported by the evaluation statics in Table 2, where E_{NS} and R^2 (ranges are from 0.8-0.83 and 0.86-0.92) are higher than that of baseflow.

Minor discrepancies between observed and simulated streamflow can be observed (Fig.6) because of differentiating baseflow and surface runoff simulations. Of course, the statistical analysis coefficient for streamflow were highest among three hydrological components, with very high E_{NS} and R^2 values beyond 0.84. Both E_{NS} and R^2 reached the “very good” criterion as described in Section 2.3.

Table 2 Evaluation statistics of monthly surface runoff, baseflow and streamflow for the Shicheng, Ningdu and Fenkeng station during calibration and validation period. “Original” refers to the SWAT original plant growth module. “Dormancy corrected” refers to the SWAT plant growth module with corrected dormancy function. “MODIS modified” refers to the modified SWAT plant growth module with the integration of MODIS LAI.

Period	Outlets	Plant growth module	Surface Runoff		Baseflow		Streamflow	
			R2	ENS	R2	ENS	R2	ENS
Calibration	Shicheng	Original	0.86	0.80	0.73	0.71	0.88	0.84
		Dormancy corrected	0.86	0.80	0.74	0.72	0.88	0.85
		MODIS modified	0.88	0.81	0.76	0.75	0.89	0.88
	Ningdu	Original	0.92	0.83	0.8	0.71	0.93	0.86
		Dormancy corrected	0.92	0.86	0.8	0.74	0.93	0.88
		MODIS modified	0.94	0.92	0.81	0.79	0.95	0.93
	Fenkeng	Original	0.91	0.80	0.78	0.74	0.93	0.93
		Dormancy corrected	0.91	0.80	0.78	0.75	0.93	0.93
		MODIS modified	0.93	0.82	0.79	0.77	0.95	0.95

Validation	Shicheng	Original	0.82	0.76	0.80	0.80	0.85	0.84
		Dormancy corrected	0.83	0.76	0.80	0.80	0.86	0.84
		MODIS modified	0.85	0.77	0.82	0.79	0.89	0.87
	Ningdu	Original	0.86	0.76	0.88	0.76	0.89	0.89
		Dormancy corrected	0.86	0.77	0.88	0.80	0.89	0.89
		MODIS modified	0.87	0.80	0.90	0.88	0.91	0.89
	Fenkeng	Original	0.90	0.77	0.89	0.76	0.91	0.83
		Dormancy corrected	0.90	0.80	0.89	0.76	0.91	0.86
		MODIS modified	0.92	0.83	0.91	0.78	0.94	0.92

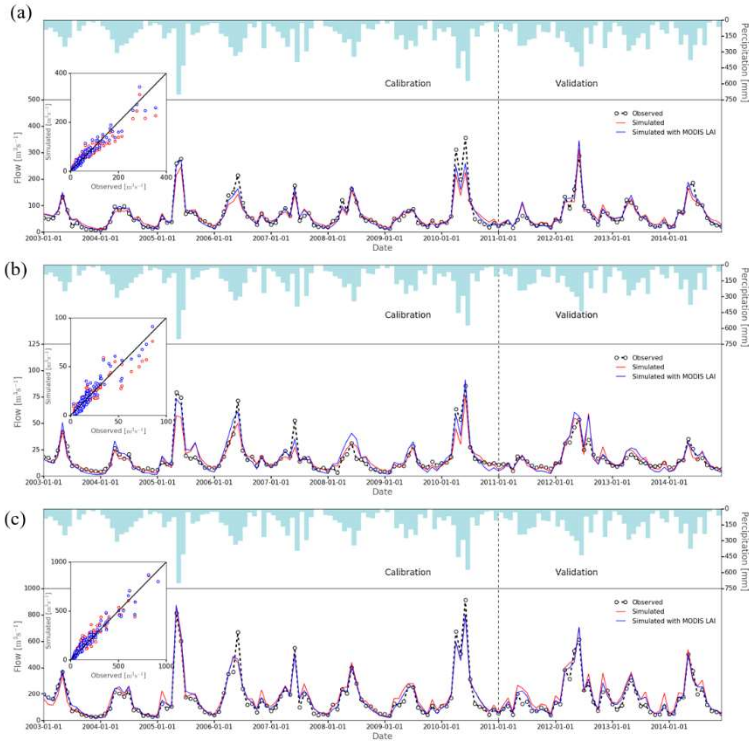

Fig.6. Temporal variability of observed and estimated monthly streamflow from original SWAT and modified SWAT with MODIS LAI at (a) Ningdu, (b) Shicheng, and (c) Fenkeng station graphical comparison of observed and simulated baseflow with original plant growth module and MODIS LAI are presented in scatter plot. Bar plot represents corresponding monthly rainfall.

Predicted flows with MODIS LAI during both the calibration and validation periods basically matched the measured flows better than the result from original SWAT plant growth module (Fig.6). This observation is supported by an apparent improvement of coefficients E_{NS} and R^2 during both calibration and validation period. For streamflow, comparison with that simulated by the original SWAT indicated that monthly flows by the MODIS LAI improved SWAT are much more aggregated and closer to identity line (or diagonal line) in all three scatter plots. Among the three hydrological stations, coefficient of Ningdu had a more obvious improvement than other two stations in the calibration period (R^2 and E_{NS} from 0.93 and 0.86 to 0.95 and 0.93, respectively), while the largest enhancement was observed at Fenkeng in the validation period (R^2 and E_{NS} from 0.91 and 0.83 to 0.94 and 0.92, respectively).

4.2.2 Sediment simulation

Based on the above streamflow results, calibration of sediment was further performed by adjusting related sensitive parameters as listed in Supplementary Material Table S4. Fig.7 shows the observed sediment and the predicted with modified MODIS LAI model and original SWAT at Fenkeng station. Overall, predicted sediment and observed sediment showed a good agreement as indicated by satisfactory values of $E_{NS} > 0.65$ and $R^2 > 0.8$ (Table 3).

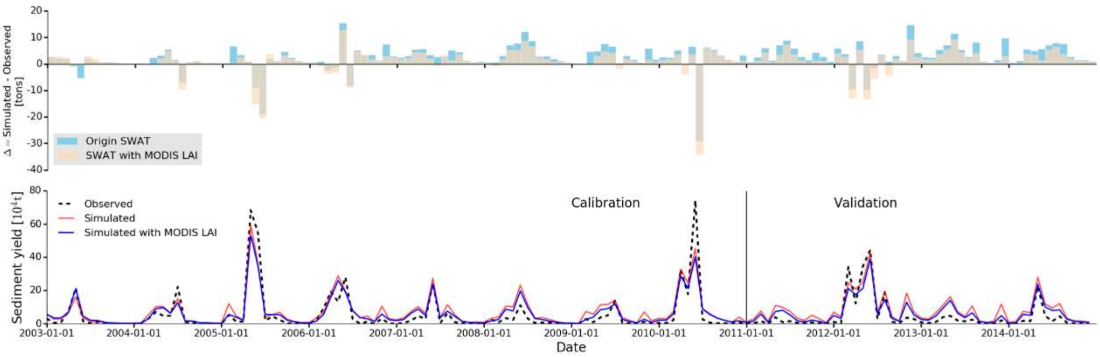

Fig.7. Temporal variability of observed and estimated monthly sediment from original SWAT and modified SWAT with MODIS LAI at Fenkeng station. Bar plot represents differences between observed sediment and simulated sediment with MODIS LAI and

original SWAT.

While comparing predicted sediment from original SWAT with that from MODIS LAI, a noticeable difference was observed in Fig.7. The values of E_{NS} and R^2 with MODIS LAI were 0.03 and 0.02 greater than original SWAT for calibration period separately, while they became 0.09 and 0.04 in validation, respectively (Table 3), suggesting an improved agreement between predicted values and observed data when integrated with MODIS LAI. Meanwhile, Scenario-2 has a middle accucracy on sediment yield prediction in comparison with Scenario-1 and Scenario-3. To further understand the mechanisms behind the temporal variability, differences between predicted and observed sediments was also generated using bar plot in Fig.7. As illustrated, there was an obvious overestimation in sediment with original SWAT. Our proposed module had a better accuracy for the most of time although it also overestimated sediment in summer and autumn months.

Table 3 Evaluation statistics of monthly sediment for the Fenkeng station during calibration and validation period. “Original” refers to the SWAT original plant growth module. “Dormancy corrected” refers to the SWAT plant growth module with corrected dormancy function. “MODIS modified” refers to the modified SWAT plant growth module with the integration of MODIS LAI.

Period	Outlets	Plant growth module	Sediment

			R2	ENS
Calibration	Fenkeng	Original	0.86	0.81
		Dormancy corrected	0.86	0.82
		MODIS modified	0.88	0.84
Validation		Original	0.80	0.66
		Dormancy corrected	0.81	0.70
		MODIS modified	0.84	0.75

To highlight the spatial distribution of modified SWAT, simulation for seasonal mean sediment yield at HRU level was computed and presented in Fig.8. Generally, the level of soil erosion risk in the Meichuan Basin was high. Dominant area of cropland experienced a high soil erosion risk with monthly mean sediment yield. A large area of forest experienced a relatively low risk due to the stronger ability of conserving soil and water. Other HRUs have moderate level of soil erosion risk, according to the soil erosion risk classification specification by the Ministry of Water Resources of China (1997). These estimates were consistent with the spatial distribution of LAI displayed in Fig.7 (details are in Section 4.1).

Although the distribution of predicted sediment seems to be reasonable, certain information was needed to better characterize the modified SWAT and to ensure accurate source area and seasonal variation of sediment. As shown in Fig.8, there is a huge variation ranging from areas with slight erosion to areas with significant soil losses in space and time. Clearly, some of the highest sediment yields were predicted during growing season (from March to June) with high rainfall. The decrease in sediment yield reflected mature of plants in July, and the developed canopy and root system reduces rill and sheet erosion (Amare et al., 2014). When LAI started to decline in November, the sediment yields had subsequently increased, especially in January and February with a lower LAI. Correspondingly, the sediment hydrographs for areas covered by different types of plants varied a lot. Indeed, sediment yield of cropland were predicted to be larger than others. On the contrary, sediment yields were lower at the border of basin where characterized with mainly forested areas and high elevations. At this point, the improved vegetation growth module with MODIS LAI could accurately identify such spatial variation of sediment simulation results.

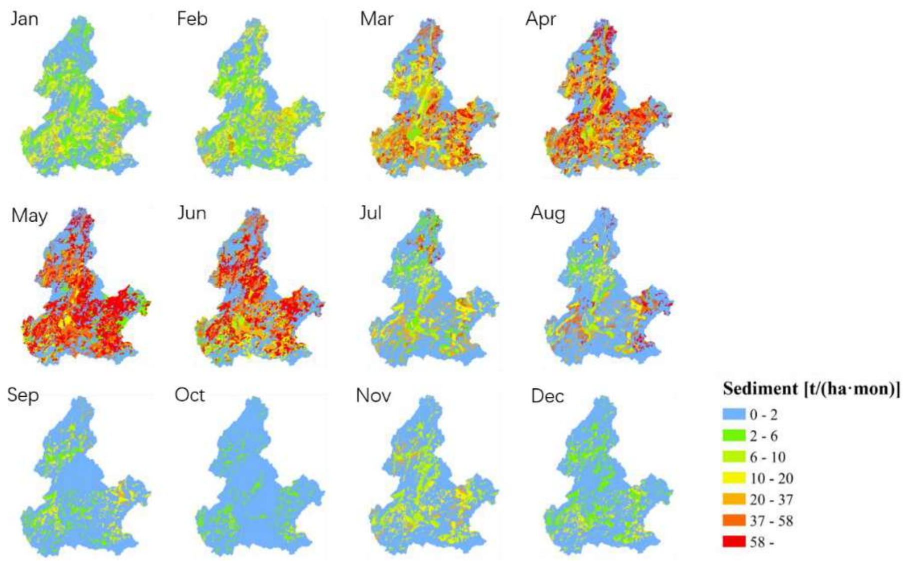

Fig.8. The average seasonal and spatial distribution of sediment at HRU level in the Meichuan Basin, as simulated by modified SWAT with MODIS LAI

4.3 Vegetation parameterizations by MODIS

4.3.1 LAI

A comparative analysis of LAI on SWAT simulation was implemented under three scenarios. The three scenarios are (1) original SWAT, (2) SWAT with corrected dormancy function, and (3) SWAT integrated with MODIS LAI. In this analysis, plants are categorized into three types according to their differences at going dormant as follows: (1) Plants which are not affected by dormancy - crop; (2) Perennials - shrub and grass; (3) Trees - evergreen, deciduous and mixed trees.

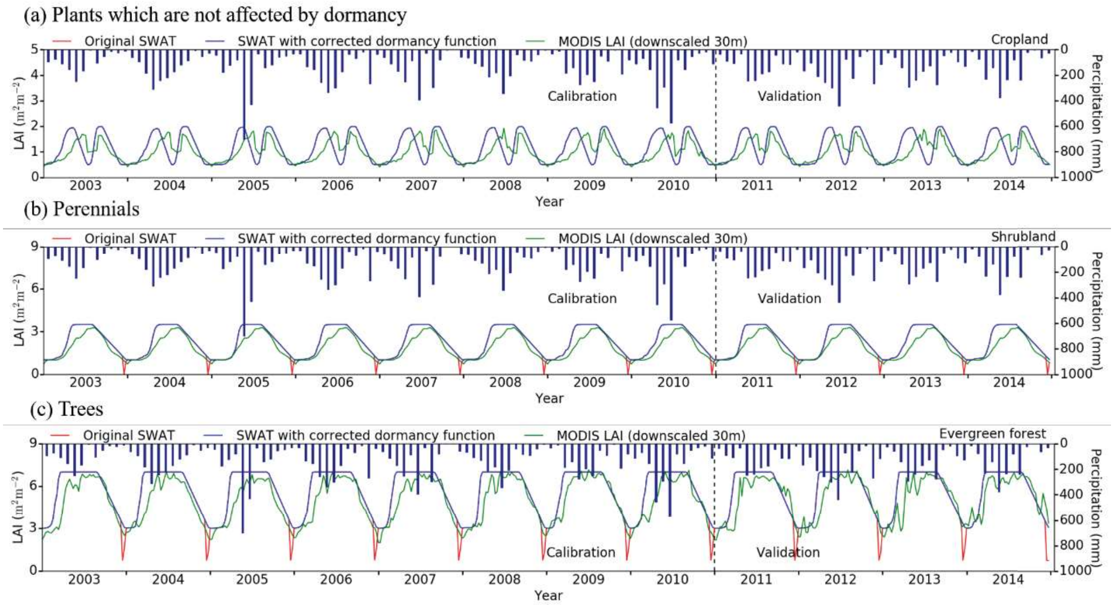

Fig.9. The LAI as simulated by original SWAT, SWAT with corrected dormancy function and modified SWAT with MODIS LAI for (a) plants which are not affected by dormancy, (b) perennials and (c) trees.

As shown in Fig.9, LAIs simulated in scenario 1 and 2 quickly reach to the peak value and occupy a very long period in its vegetation growth cycle if comparing with the observed LAI in scenario 3. This indicates that the simulated vegetation in scenario 1 and 2 results in an overestimated transpiration and consequently leads to an underestimated streamflow rather than in scenario 3. In scenario 1 and 2, simulated vegetation LAI peaks always appear earlier than rainfall peaks about one month in time series, while MODIS LAI peaks lag behind rainfall peaks around 2~4 weeks depending on vegetation types in scenario 3. Such mismatch of two peaks in original vegetation growth module apparently causes the system error of SWAT and low predictable accuracy on simulation.

4.3.2 Parameter C

Soil erosion and sediment yield in SWAT are modelled using a Modified Universal Soil Loss Equation (MUSLE). Plant growth module plays an important role in simulating the cover and management factor (C factor) in MUSLE. The changes of C factor were analyzed for six plant types between the improved and original model, and the impact of plant and ground cover on soil loss was hereby investigated as shown in Fig.10.

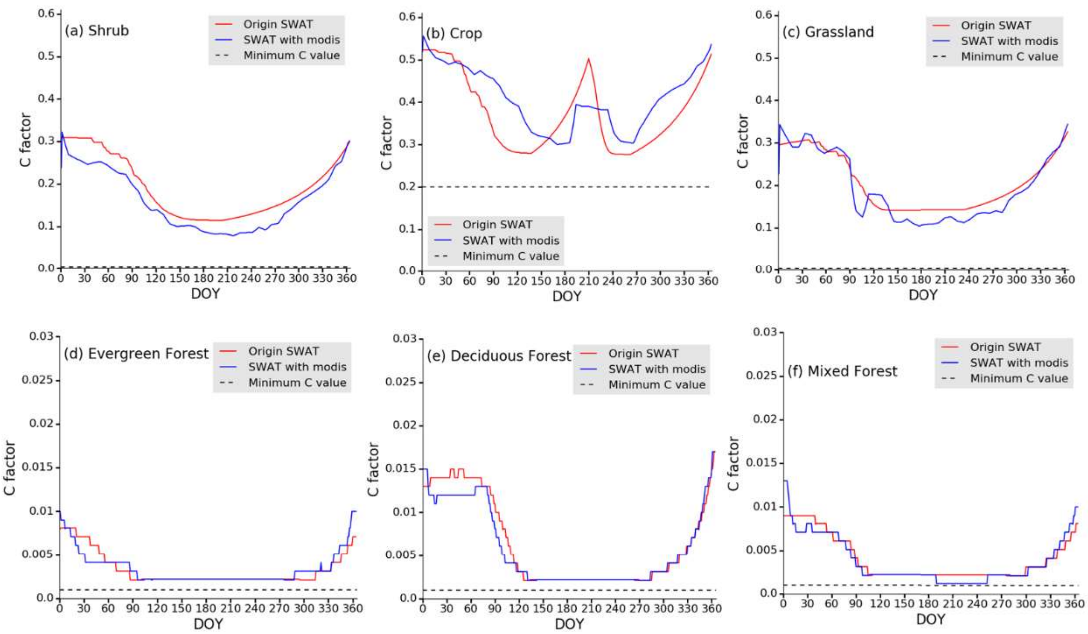

Fig.10. Comparison of C factor simulated by original SWAT and modified SWAT with MODIS LAI for (a) shrub, (b) cropland, (c) grassland, (d) evergreen forest, (e) deciduous

forest and (f) mixed forest. The horizontal black dash line marks the minimum C value defined in SWAT plant database

For crop, the mismatch of C values between SWAT with MODIS LAI and original SWAT is so obvious. During growing season, there is a drastic change of C values within a year in the original SWAT and such sudden peaks of C factor may produce extremely high sediment yield in certain periods. The curve of C values from MODIS LAI fits well with crop growth patterns, particularly illustrating distinct one-month fallow period between two cropping seasons. It is much more acceptable than simulated by original SWAT. For shrub and grass, mean value of C factor simulated with MODIS LAI were lower than original SWAT. For evergreen, deciduous and mixed forest, there were no significant differences between the two C factors. From the above comparison, C factor estimated by SWAT with MODIS LAI captured the vegetation dynamics well, illustrating that the C factor values estimated by the SWAT with MODIS LAI are temporally consistent and reasonable.

5 Discussion

5.1 Changes of remotely sensed LAI on different scales

Based on the results of this study, the performance of remotely sensed LAI on SWAT is related to two main scale issues. Firstly, due to the coarse resolution of original MODIS LAI products (500m), mixed pixels are often presented in this gridding system that cannot provide insufficient spatial details of vegetation (Ichiba, 2016; Gires et al., 2017). Another major issue is the relationship between SWAT-HRU and MODIS LAI pixel, producing mismatch on the border of HRU as indicated in Fig.11 (Rafieeinasab et al., 2015; Salvadore et al., 2015; Ichiba et al., 2018). With these two issues, the time series of MODIS LAI values aggregated at HRU level had a massive change on different scales. As shown in Fig.4, the LAI time series of crop (30m) displayed a double-cropping pattern in subtropics instead of a wrong single-cropping pattern (500m) after our time filtering and downscaling.

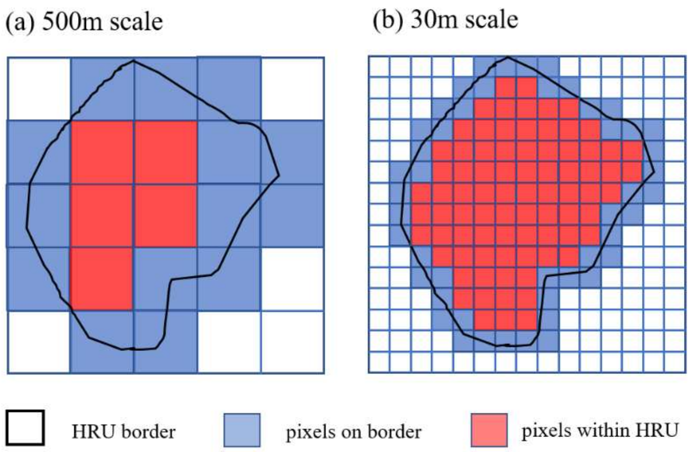

Fig.11 Graphic representation of the (a) 500m-scale and (b) 30m-scale mismatch between SWAT-HRU and MODIS LAI pixel in the border of HRU.

The average size of HRUs in this work is 15.13 km^2. As shown in Fig.11, high resolution MODIS LAI (30m) produce less mismatched area than the original MODIS LAI (500m). The larger pixel size of MODIS causes a bigger vegetation mixed area nearby SWAT-HRU borders and the aggregation of LAI at HRUs absolutely result in LAI converging between two neighbor HRU areas although these HRUs have different vegetation types.

We considered the characteristics of the MODIS LAI variation at different scales and processed the MODIS LAI product to precisely reflect ground truth of cropping in subtropics. So MODIS LAI was able to be properly aggregated to SWAT-HRU and improved the accuracy of SWAT simulation.

5.2 Improved SWAT eco-hydrological processes with satellite-observed MODIS LAI

Spatially distributed watershed models such as SWAT in subtropical areas can greatly benefit from high resolution LAI estimates provided by our enhanced method. Compared with SWAT-simulated LAI value, satellite- observed LAI values have a great improvement in spatial details and recognize cropping pattern in time more clearly (Yuan et al., 2011). In SWAT, several subroutines such as etact.f (calculating actual evapotranspiration) and cfactor.f (calculating C factor for sediment simulation) request LAI data (Neitsch et al., 2011). The enhancements of LAI by MODIS are definitely delivered to streamflow and sediment yield through by these model chaining (Table 2 and 3). In general, these enhancements may be catalogued into three eco-hydrological processes as follows:

(1) Canopy interception loss. Cui et al. (2015) reported that interception loss is an important component of the regional water balance and even make up 30% of rainfall during rainy season in tropical or subtropical vegetation covered areas. The peak of MODIS LAI showed a better agreement with precipitation in comparison with simulated LAI (Fig.9), correspondingly the interception loss related with rainfall was estimated by SWAT more accurately after incorporating MODIS LAI.

(2) Soil water content. Evapotranspiration occurs from a SWAT-HRU area covered with growing vegetation that has access to soil water and vary from day to day as a function of LAI in SWAT (Gao et al., 2008). Therefore, the improvement of LAI would be reflected to some degree in soil water content due to an increase accuracy of simulated evapotranspiration.

(3) Sediment yield. In SWAT, C factor is a comprehensive function of above-ground biomass, residue on the soil surface and the minimum C factor for the plant (Song et al., 2011). Except for minimum C factor derived from crop database, both biomass and residue are calculated by the time series of LAI. So estimating sediment yield by MULSE may also benefit from an improved MULSE C factor too.

5.3 The nature of vegetation growth model in SWAT

As shown in Fig.9, the LAI curves of all plants reached the peak quickly (the maximum of LAI) at the beginning of growing season by the original SWAT. We could not obtain an appropriate LAI curve that reasonably describes vegetation dynamics as the MODIS LAI presented even the SWAT parameters had been adjusted to keep plant growth at the slowest speed. This could be attributed to the EPIC model used in SWAT that is only adaptable to a temperate zone (Alemayehu et al., 2017).

Temperature is the most important controlling factor for governing plant growth in EPIC. In the temperate zones, the temperature when seeding is around 10~15℃ and rises to 30~35℃ after 2~3 months before harvesting (Bai et al., 2018). Considering the plant growth pattern in the temperate zone, the accumulation of heat units is slow, especially at the beginning of plant growing (Neitsch et al., 2011). However, there is an extremely rapid accumulation of heat units in tropics and subtropics due to high temperature throughout the whole year, resulting an incredible rapid LAI increase at the beginning of growing season in SWAT-EPIC.

The good match on time between satellite-observed MODIS LAI and rainfall shown in Fig.9 demonstrated the nature of vegetation growth in subtropics controlled by rainfall, not temperature. Furthermore, vegetation in temperate zone such as forest have a dormant period at winter with low temperature by the original SWAT but not in tropics and subtropics by MODIS improved model (Trybula et al., 2015). All the above reminds using satellite observed MODIS LAI rather than SWAT-simulated LAI may lead to a better performance of SWAT in subtropical area.

6 Conclusions

Modelling vegetation growth is of great importance for simulating streamflow and sediment in hydrological model. SWAT-EPIC plant growth model using a heat-accumulation function is just applicable to plants in temperate zones, where temperature dominates plant growth. However, vegetation growth in subtropics is mainly controlled by precipitation. SWAT fails to simulate an accurate vegetation growth and inevitably caused the errors on vegetation-derived succeeding factors. Assuming that satellite-observed MODIS LAI values represent the real scenario of land cover, we integrated our downscaled high-quality MODIS LAI time series data into modified SWAT plant growth module. As shown in the demonstration area, the SWAT reached a great accuracy on the validation of streamflow (E_{NS}= 0.92 and R^2 =0.94) and sediment yield (E_{NS}= 0.75 and R^2 =0.84) and achieved a remarkable improvement on its applicability in subtropics as follows:

(1) High spatiotemporal resolution LAIs that substantially match SWAT-HRUs were generated with MODIS. It reflects the correct relation between the LAI curves of plant growth and precipitation in subtropical regions. Meanwhile, cropping pattern and spatial details of crops were appropriately represented, namely, two-season cropping in subtropics instead of sing-season cropping. Inappropriate dormancy was also avoided.

(2) The applicability of SWAT in subtropics was significantly improved by integrating an improved MODIS LAI into modified SWAT plant growth model. The high quality of refined LAIs on SWAT-HRUs were broadcasted into subsequent SWAT modules. More accurate LAI-related factors like canopy, interception loss, evapotranspiration and C factor are derived in SWAT and lead to a definitely higher accuracy on the prediction of streamflow and sediment yields.

(3) The drawbacks or limitation of SWAT-EPIC plant growth model in tropics or subtropics were figured out through by analyzing the time series of LAI data simulated by the original SWAT and derived by MODIS LAI. The growth model by the accumulation of heat units in growing season is not effective in tropical or subtropical zones as in temperate zones.

Modified SWAT we proposed using MODIS LAI presents an attractive applicability in subtropics and meanwhile shows a high universality. It does not request additional field measurement and no more specific satellite data processing as the MODIS MCD15A2H is a long-term and stale product that observes globe every 8 days at 500-meters resolution.

Acknowledgements

This study was supported by National Key Research and Development Program of China (No. 2017YFB0503702 and No. 2016YFC0503602), National Natural Science Foundation of China (No. 41771435 and No. 41201038), China Scholarship Council (No. 201704910297), Guangxi Science and Technology Major Project (No. GK-AA17202033) and CAS Huairou Eco-Environmental Observatory. Special thanks to Junzhi Liu for providing the hydrological observed data and technical support for this study.

References

Abbaspour, K.C., Yang, J., Maximov, I., Siber, R., Bogner, K., Mieleitner, J., Zobrist, J., and Srinivasan, R. (2007). Modelling hydrology and water quality in the pre-alpine/ alpine Thur watershed using SWAT. Journal of Hydrology. 333, 413–430.

Abbaspour, K. C., Rouholahnejad, E., Vaghefi, S., Srinivasan, R., Yang, H., and Kløve, B. (2015). A continental-scale hydrology and water quality model for europe: calibration and uncertainty of a high-resolution large-scale swat model. Journal of Hydrology, 524, 733-752.

Alemayehu, T., Van Griensven, A., Taddesse Woldegiorgis, B., and Bauwens, W. (2017). An improved swat vegetation growth module and its evaluation for four tropical ecosystems. Hydrology & Earth System Sciences, 21(9), 1-32.

Almeida, C., Chambel-Leitão, P., and Jauch, E. (2011). SWAT LAI calibration with local LAI measurements. International Swat Conference & Worshops.

Amare, T., Zegeye, A. D., Yitaferu, B., Steenhuis, T. S., Hurni, H., & Zeleke, G. (2014). Combined effect of soil bund with biological soil and water conservation measures in the northwestern ethiopian highlands. Ecohydrology & Hydrobiology, 14(3), 192-199.

Andersen, J., Dybkjaer, G., Jensen, K. H., Refsgaard, J. C., and Rasmussen, K. (2002). Use of remotely sensed precipitation and leaf area index in a distributed hydrological model. Journal of Hydrology, 264(1–4), 34-50.

Arnold, J. G., Srinivasan, R., Muttiah, R. S., and Williams, J. R. (1998). Large area hydrologic modeling and assessment part I: model development, JAWRA Journal of the American Water Resources Association, 34(1): 73-89.

Arnold, J. G., Moriasi, D. N., Gassman, P. W., Abbaspour, K. C.,White, M. J., Srinivasan, R., Santhi, C., Harmel, R. D., van Griensven, A., Van Liew, M. W., Kannan, N., and Jha, M. K. (2012). SWAT: Model Use, Calibration, and Validation. Transactions of the Asabe, 55, 1491–1508.

Bai, P., Liu, X., Zhang, Y., & Liu, C. (2018). Incorporating vegetation dynamics noticeably improved performance of hydrological model under vegetation greening. Science of the Total Environment, 643, 610-622.

Berghuijs, W. R., Sivapalan, M., Woods, R. A., and Savenije, H. H. G. (2015). Patterns of similarity of seasonal water balances: a window into streamflow variability over a range of time scales. Water Resources Research, 50(7), 5638–5661.

Bressiani, D. de A., Gassman, P. W., Fernandes, J. G., Garbossa, L. H. P., Srinivasan, R., Bonumá, N. B., and Mendiondo, E. M. (2015). A review of soil and water assessment tool (SWAT) applications in Brazil: Challenges and prospects. International Journal of Agricultural and Biological Engineering, 8, 1–27.

Chen, J., Jönsson, P., Tamura, M., Gu, Z., Matsushita, B., and Eklundh, L. (2004). A simple method for reconstructing a high-quality ndvi time-series data set based on the savitzky–golay filter. Remote Sensing of Environment, 91(3–4), 332-344.

Cui, Y., Jia, L., Hu, G., & Zhou, J. (2015). Mapping of interception loss of vegetation in the heihe river basin of china using remote sensing observations. IEEE Geoscience and Remote Sensing Letters, 12(1), 23-27.

Emelyanova, I. V., Mcvicar, T. R., Niel, T. G. V., Ling, T. L., & Dijk, A. I. J. M. V. (2013). Assessing the accuracy of blending landsat–modis surface reflectances in two landscapes with contrasting spatial and temporal dynamics: a framework for algorithm selection. Remote Sensing of Environment, 133(12), 193-209.

Fang, H., Liang, S., Townshend, J. R., and Dickinson, R. E. (2008). Spatially and temporally continuous LAI data sets based on an integrated filtering method: examples from north America. Remote Sensing of Environment, 112(1), 75-93.

Francesconi, W., Srinivasan, R., Pérez-Miñana, E., Willcock, S. P., and Quintero, M. (2016). Using the soil and water assessment tool (SWAT) to model ecosystem services: a systematic review. Journal of Hydrology, 535, 625-636.

Gao, F., Masek, J., Schwaller, M., and Hall, F. (2006). On the blending of the landsat and modis surface reflectance: predicting daily landsat surface reflectance. IEEE Transactions on Geoscience & Remote Sensing, 44(8), 2207-2218.

Giambelluca, T. W., Scholz, F. G., Bucci, S. J., Meinzer, F. C., Goldstein, G., Hoffmann, W. A., Franco, A. C., and Buchert, M. P. (2009). Evapotranspiration and energy balance of Brazilian savannas with contrasting tree density. Agricultural and Forest Meteorology, 149, 1365–1376.

Gires, A., Tchiguirinskaia, I., Schertzer, D., Ochoa-Rodriguez, S., & Veldhuis, M. C. T. (2017). Fractal analysis of urban catchments and their representation in semi-distributed models: imperviousness and sewer system. Hydrology and Earth System Sciences, 21(5), 2361-2375.

Glavan, M., Pintar, M., and Urbanc, J. (2015). Spatial variation of crop rotations and their impacts on provisioning ecosystem services on the river Drava alluvial plain. Sustainability of Water Quality & Ecology, 5, 31–48.

Gong, P., Wang, J., Yu, L., Zhao, Y., Zhao, Y., Liang, L. & Li, C. (2013). Finer resolution observation and monitoring of global land cover: First mapping results with Landsat TM and ETM+ data. International Journal of Remote Sensing, 34(7), 2607-2654.

Guzha, A. C., Rufino, M. C., Okoth, S., Jacobs, S., & Nóbrega, R.L.B. (2018). Impacts of land use and land cover change on surface runoff, discharge and low flows: evidence from east africa. Journal of Hydrology Regional Studies, 15(15), 49-67.

Hilker, T., Lyapustin, A. I., Tucker, C. J., Hall, F. G., Myneni, R. B., & Wang, Y., et al. (2014). Vegetation dynamics and rainfall sensitivity of the amazon. Proc Natl Acad Sci USA, 111(45), 16041-16046.

Houborg, R., Mccabe, M. F., & Gao, F. (2016). A spatio-temporal enhancement method for medium resolution LAI (STEM-LAI). International Journal of Applied Earth Observation & Geoinformation, 47, 15-29.

Ichiba, A.: X-band radar data and predictive management in urban hydrology, Ph.D. thesis, Universite Paris-Est, 2016.

Ichiba, A., Gires, A., Tchiguirinskaia, I., Schertzer, D., Bompard, P, & Veldhuis, M. C. T. (2018). Scale effect challenges in urban hydrology highlighted with a distributed hydrological model. Hydrology & Earth System Sciences, 22(1), 1-25.

Jolly, W. M., & Running, S. W. (2004). Effects of precipitation and soil water potential on drought deciduous phenology in the Kalahdari. Global Change Biology, 10, 303–308.

Jarihani, A.A., McVicar, T.R., Van Niel, T.G., Emelyanova, I.V., Callow, J.N. & Johansen, K. (2014). Blending landsat and modis data to generate multispectral indices: a comparison of ``index-then-blend'' and ``blend-then-index'' approaches. Remote Sensing, 6(10), 9213-9238.

Kauffman, S., Droogers, P., Hunink, J., Mwaniki, B., Muchena, F., Gicheru, P., Bindraban, P., Onduru, D., Cleveringa, R., & Bouma, J. (2014). Green Water Credits–exploring its potential to enhance ecosystem services by reducing soil erosion in the Upper Tana basin, Kenya. International Journal of Biodiversity Science Ecosystem Services & Management, 10 (2), 133–143.

Kiniry, J. & MacDonald, J. (2008). Plant growth simulation for landscape-scale hydrological modelling.

International Association of Scientific Hydrology Bulletin, 53(5), 1030–1042.

Knyazikhin, Y., Martonchik, J. V., Myneni, R. B., Diner, D. J., & Running, S. W. (1998). Synergistic algorithm for estimating vegetation canopy leaf area index and fraction of absorbed photosynthetically active radiation from MODIS and MISR data. Journal of Geophysical Research, 103(D24), 32257–32276.

Li, D., Pan, M., Cong, Z., Zhang, L., & Wood, E. (2013). Vegetation control on water and energy balance within the budyko framework. Water Resources Research, 49(2), 969-976.

Li, H. X., Zhang, Y. Q., Chiew, F. H. S., & Xu, S. G. (2009). Predicting runoff in ungauged catchments by using xinanjiang model with modis leaf area index. Journal of Hydrology, 370(1), 155-162.

Li, M. M. (2013). Study of developing a core collection for jiangxi traditional rice germplasm by using ssr markers. Journal of Plant Genetic Resources, 13(6), 952-957(6).

Li, R., Zhu, A-X., Song, X., Li, B., Pei, T., & Qin, C. (2012). Effects of spatial aggregation of soil spatial information on watershed hydrological modelling. Hydrological Processes, 26(9), 1390-1404.

Liu, J., Gao, G., Wang, S., Lei, J., Wu, X., & Fu, B. (2018). The effects of vegetation on runoff and soil loss: multidimensional structure analysis and scale characteristics. Journal of Geographical Sciences, 28(1), 59-78.

Lychuk, T. E., Izaurralde, R. C., Hill, R. L., Mcgill, W. B., & Williams, J. R. (2015). Biochar as a global change adaptation: predicting biochar impacts on crop productivity and soil quality for a tropical soil with the environmental policy integrated climate (EPIC) model. Mitigation & Adaptation Strategies for Global Change, 20(8), 1437-1458.

Mekonnen, D. F., Duan, Z., Rientjes, T., & Disse, M. (2017). Analysis of the combined and single effects of LULC and climate change on the streamflow of the upper Blue Nile river basin (UBNRB): using statistical trend tests, remote sensing landcover maps and the swat model. Hydrology & Earth System

Sciences Discussions, 1-26.

Ministry of Water Resources of China. 1997. Soil Erosion Risk Classification Specification (SL190–1996). China Water Power Press: Beijing, China; 2–16.

Moriasi, D. N., Arnold, J. G., Liew, M. W. V., Bingner, R. L., Harmel, R. D., & Veith, T. L. (2007). Model evaluation guidelines for systematic quantification of accuracy in watershed simulations. Transactions of the Asabe, 50(3), 885-900.

Mwangi, H. M., Julich, S., Patil, S. D., Mcdonald, M. A., & Feger, K. (2016). Modelling the impact of agroforestry on hydrology of Mara river basin in east Africa. Hydrological Processes, 30(18), 3139-3155.

Naseem, B., Ajami, H., Yi, L., Cordery, I., & Sharma, A. (2016). Multi-objective assessment of three remote sensing vegetation products for streamflow prediction in a conceptual ecohydrological model. Journal of Hydrology, 543, 686-705.

Nash, J. E., & Sutcliffe, J. V. (1970). River flow forecasting through conceptual models part I—A discussion of principles. Journal of hydrology, 10(3), 282-290.

Neitsch, S. L., Arnold, J. G., Kiniry, J. R., Srinivasan, R., & Williams, J. R. (2011). Soil and water assessment tool input/output file documentation: version 2009. texas water resources institute technical report 365. Journal of Information Processing & Management, 33.

Nourani, V., Fard, A. F., Gupta, H. V., Goodrich, D. C., & Niazi, F. (2017). Hydrological model parameterization using NDVI values to account for the effects of land cover change on the rainfall–runoff response. Hydrology Research, 48(6), 1455-1473.

Pfeifer, M., Lefebvre, V., Gonsamo, A., Pellikka, P. K. E., Marchant, R., Denu, D., & Platts, P. J. (2014). Validating and linking the GIMMS leaf area index (LAI3g) with environmental controls in tropical Africa. Remote Sensing, 6, 1973–1990.

Plesca, I., Timbe, E., Exbrayat, J. F., Windhorst, D., Kraft, P., Crespo, P., Vaché, K., Frede, H. G., Breuer, L. (2012). Model inter comparison to explore catchment functioning: results from a remote montane tropical rainforest. Ecological Modelling. 239, 3–13.

Qiao, L., Zou, C. B., Will, R. E., & Stebler, E. (2015). Calibration of swat model for woody plant encroachment using paired experimental watershed data. Journal of Hydrology, 523, 231-239.

Rafieeinasab, A., Norouzi, A., Kim, S., Habibi, H., & Nazari, B., et al. (2015). Toward high-resolution flash flood prediction in large urban areas – analysis of sensitivity to spatiotemporal resolution of rainfall input and hydrologic modeling. Journal of Hydrology, 531, 370-388.

Ren, J., Yu, F., Qin, J., Chen, Z., & Tang, H. (2010). Integrating remotely sensed LAI with epic model based on global optimization algorithm for regional crop yield assessment. IEEE Geoscience and Remote Sensing Symposium (Vol.38, pp.2147-2150).

Salvadore, E., Bronders, J., & Batelaan, O. (2015). Hydrological modelling of urbanized catchments: a review and future directions. Journal of Hydrology, 529, 62-81.

Santhi, C., Arnold, J. G., Williams, J. R., Dugas, W. A., Srinivasan, R., & Hauck, L. M. (2001). Validation of the swat model on a large river basin with point and nonpoint sources. JAWRA Journal of the American Water Resources Association, 37(5), 1169–1188.

Savitzky, A., & Golay, M. J. E. (1964). Smoothing and differentiation of data by simplified least squares procedures. Analytical Chemistry, 36, 1627– 1639.

Song, X., Duan, Z., Kono, Y., & Wang, M. (2011). Integration of remotely sensed C factor into swat for modelling sediment yield. Hydrological Processes, 25(22), 3387-3398.

Starks, P. J., & Moriasi, D. N. (2009). Spatial resolution effect of precipitation data on swat calibration and performance: implications for ceap. Transactions of the ASABE, 52(4), 1171-1180.

Stephenson, N. (1998). Actual evapotranspiration and deficit: biologically meaningful correlates of vegetation distribution across spatial scales. Journal of Biogeography, 25(5), 16.

Strauch, M., & Volk, M. (2013). SWAT plant growth modification for improved modeling of perennial vegetation in the tropics. Ecological Modelling, 269(1771), 98-112.

Sun, W., Fan, J., Wang, G., Ishidaira, H., Bastola, S., & Yu, J., et al. (2018). Calibrating a hydrological model in a regional river of the qinghai–tibet plateau using river water width determined from high spatial resolution satellite images. Remote Sensing of Environment, 214, 100-114.

Trybula, E. M., Cibin, R., Burks, J. L., Chaubey, I., Brouder, S. M., & Volenec, J. J. (2015). Perennial rhizomatous grasses as bioenergy feedstock in swat: parameter development and model improvement. Global Change Biology Bioenergy, 7(6), 1185-1202.

Wagner, P. D., Kumar, S., Fiener, P. & Schneider, K. (2011). Hydrological Modeling with SWAT in a Monsoon-Driven environment: Experience from the Western Ghats, India. Transactions of the Asabe, 54, 1783– 1790.

Weiss, M., Baret, F., Garrigues, S., & Lacaze, R. (2007). LAI and fAPAR CYCLOPES global products derived from vegetation. part 2: validation and comparison with MODIS collection 4 products. Remote Sensing of Environment, 110(3), 317-331.

Williams, J. R., Jones, C. A., Kiniry, J. R., Spanel, D. A. (1989). The EPIC crop growth model. Transactions of the Asabe, 32, 497–511.

Wischmeier, W. H., & Smith, D. D. (1978). Predicting rainfall erosion losses - a guide to conservation planning. Agric Handbook, 537.

Yang, D., Shao, W., Yeh, J. F., Yang, H., Kanae, S., & Oki, T. (2009). Impact of vegetation coverage on regional water balance in the nonhumid regions of china. Water Resources Research, 45(7), 450-455.

Tuo, Y., Marcolini, G., Disse, M., & Chiogna, G. (2018). A multi-objective approach to improve swat model calibration in alpine catchments. Journal of Hydrology, 559, 347-360.

Yuan, H., Dai, Y., Xiao, Z., Ji, D., & Shangguan, W. (2011). Reprocessing the MODIS leaf area index products for land surface and climate modelling. Remote Sensing of Environment, 115(5), 1171-1187.

Zhang, Y., & Wegehenkel, M. (2006). Integration of MODIS data into a simple model for the spatial distributed simulation of soil water content and evapotranspiration. Remote sensing of Environment, 104(4), 393-408.

Zhang, Y., Chiew, F. H., Zhang, L., & Li, H. (2009). Use of remotely sensed actual evapotranspiration to improve rainfall–runoff modeling in Southeast Australia. Journal of Hydrometeorology, 10(4), 969-980.

Zhao, H. G., Yang, S. T., & Huang, Y. C. (2018). Utilizing the MODIS-derived leaf area index to investigate the impact of vegetation processes on hydrological simulation of macroscale catchment. Environmental Earth Sciences, 77(1), 11.

Zhou, J., He, D., Xie, Y., Liu, Y., & Yang, Y., et al. (2015). Integrated swat model and statistical downscaling for estimating streamflow response to climate change in the lake dianchi watershed, china. Stochastic Environmental Research & Risk Assessment, 29(4), 1193-1210.

Zhou, Y., Zhang, Y., Vaze, J., Lane, P., & Xu, S. (2013). Improving runoff estimates using remote sensing vegetation data for bushfire impacted catchments. Agricultural and forest meteorology, 182, 332-341.

Zhu, A. X., Hudson, B., Burt, J., Lubich, K., & Simonson, D. (2001). Soil mapping using GIS, expert knowledge, and fuzzy logic. Soil Science Society of America Journal, 65(5), 1463–1472.